Virulence Meets Metabolism: Cra and KdpE Gene Regulation in Enterohemorrhagic *Escherichia coli*

Jacqueline W. Njoroge, Y. Nguyen, Meredith M. Curtis, Cristiano G. Moreira, and Vanessa Sperandio

Departments of Microbiology and Biochemistry, University of Texas Southwestern Medical Center, Dallas, Texas, USA

ABSTRACT **Gastrointestinal (GI) bacteria sense diverse environmental signals as cues for differential gene regulation and niche adaptation. Pathogens such as enterohemorrhagic *Escherichia coli* (EHEC), which causes bloody diarrhea, use these signals for the temporal and energy-efficient regulation of their virulence factors. One of the main virulence strategies employed by EHEC is the formation of attaching and effacing (AE) lesions on enterocytes. Most of the genes necessary for the formation of these lesions are grouped within a pathogenicity island, the locus of enterocyte effacement (LEE), whose expression requires the LEE-encoded regulator Ler. Here we show that growth of EHEC in glycolytic environments inhibits the expression of *ler* and consequently all other LEE genes. Conversely, growth within a gluconeogenic environment activates expression of these genes. This sugar-dependent regulation is achieved through two transcription factors: KdpE and Cra. Both Cra and KdpE directly bind to the *ler* promoter, and Cra's affinity to this promoter is catabolite dependent. Moreover, we show that the Cra and KdpE proteins interact *in vitro* and that KdpE's ability to bind DNA is enhanced by the presence of Cra. Cra is important for AE lesion formation, and KdpE contributes to this Cra-dependent regulation. The deletion of *cra* and *kdpE* resulted in the ablation of AE lesions. One of the many challenges that bacteria face within the GI tract is to successfully compete for carbon sources. Linking carbon metabolism to the precise coordination of virulence expression is a key step in the adaptation of pathogens to the GI environment.**

IMPORTANCE **An appropriate and prompt response to environmental cues is crucial for bacterial survival. Cra and KdpE are two proteins found in both nonpathogenic and pathogenic bacteria that regulate genes in response to differences in metabolite concentration. In this work, we show that, in the deadly pathogen enterohemorrhagic *Escherichia coli* (EHEC) O157:H7, which causes bloody diarrhea, these two proteins influence important virulence traits. We also propose that their control of one or more of these virulence traits is due to the direct interaction of the Cra and KdpE proteins with each other, as well as with their DNA targets. This work shows how EHEC coopts established mechanisms for sensing the metabolites and stress cues in the environment, to induce virulence factors in a temporal and energy-efficient manner, culminating in disease. Understanding how pathogens commandeer nonpathogenic systems can help us develop measures to control them.**

Received 9 August 2012 **Accepted** 12 September 2012 **Published** 16 October 2012

Citation Njoroge JW, Nguyen Y, Curtis MM, Moreira CG, Sperandio V. 2012. Virulence meets metabolism: Cra and KdpE gene regulation in enterohemorrhagic *Escherichia coli*. mBio 3(5):e00280-12. doi:10.1128/mBio.00280-12

Editor Philippe Sansonetti, Institut Pasteur

Copyright © 2012 Njoroge et al. This is an open-access article distributed under the terms of the Creative Commons Attribution-Noncommercial-Share Alike 3.0 Unported License, which permits unrestricted noncommercial use, distribution, and reproduction in any medium, provided the original author and source are credited.

Address correspondence to Vanessa Sperandio, vanessa.sperandio@utsouthwestern.edu.

One of the major challenges faced by bacteria within communities is acquisition of carbon and nitrogen to synthesize primary metabolites. The mammalian gastrointestinal (GI) tract harbors trillions of indigenous bacteria of approximately 1,000 different species (1), whose coexistence relies on the ability of each member to utilize one or a few limiting resources. Invading pathogens have to compete with the microbiota for these resources to establish colonization. These pathogens tend to be aggressive and greedy in their search for a colonization niche and achieve this purpose by precisely coordinating expression of an arsenal of virulence genes.

The GI pathogen enterohemorrhagic *Escherichia coli* (EHEC) causes hemorrhagic colitis and hemolytic-uremic syndrome (HUS) (2). EHEC employs a type 3 secretion system (T3SS), a needle-like structure through which effectors are translocated into host cells. The T3SS is responsible for the attachment of EHEC to the gut epithelium and the induction of extensive actin rearrangement in the host epithelial cells, culminating in the formation of attaching and effacing (AE) lesions (pedestal-like structures) (2). Most of the genes necessary for their formation are contained within a pathogenicity island (PI) known as the locus of enterocyte effacement (LEE) (2). The majority of the LEE genes are grouped into five major operons, *LEE1* to *LEE5*, and encode the structural components of the T3SS, as well as some of the effectors. The *ler* gene encodes the master regulator of the LEE genes and is essential for the secretion of LEE and non-LEE-encoded T3SS effectors, pedestal formation, and overall virulence in EHEC (2–5). Expression of *ler* is regulated by numerous transcription factors, including the response regulator (RR) KdpE (4, 6). KdpE is phosphorylated by its cognate histidine sensor kinase (HK) KdpD in response to potassium and osmotic stress. KdpD and KdpE are encoded within the same operon and regulate the *kdpFABC* genes

important for K^+ transport and general bacterial homeostasis (7–9). KdpE is also phosphorylated by the noncognate HK QseC in response to the host hormones epinephrine and norepinephrine and a signaling molecule, autoinducer-3 (AI-3), produced by the GI microbiota (6, 10–13, 31, 58). The high level of control of *ler* expression ensures that, in response to diverse environmental signals, EHEC is able to tightly regulate the expression of the LEE and its virulence.

One important environmental signal that bacteria respond to is carbon nutrients. EHEC's ability to initiate growth and maintain colonization *in vivo* depends on whether the carbon source is glycolytic or gluconeogenic (14–17). *In vitro* studies showed that metabolites can regulate the expression of both metabolism and nonmetabolism genes. The catabolite repressor/activator protein Cra (also known as FruR, a member of the LacI family) is a transcription factor that uses fluctuations in sugar concentrations to activate or inhibit expression of its target genes (18). Cra regulates virulence in *Salmonella enterica* and *Shigella flexneri* (19, 20). Cra's function is cyclic AMP (cAMP) independent but is inhibited by the presence of micromolar concentrations of fructose-1-phosphate (F1P) or millimolar amounts of fructose-1,6-bisphosphate (FBP) (21, 22). These metabolic intermediates bind to the inducer binding domain of Cra, decreasing its binding affinity for target promoters and consequently decreasing its regulatory function.

Here we show that KdpE regulation of *ler* is glucose dependent and that this dependency is through Cra. We show that Cra and KdpE directly interact with each other to promote *ler* transcription and AE lesion formation. This convergence of regulation by Cra and KdpE introduces a novel mechanism of regulation that links metabolism to pathogenesis.

RESULTS AND DISCUSSION

Carbon regulation of EHEC pathogenesis. Given the key role that carbon sources play within the GI tract for niche competition, we investigated the role that carbon sources have in EHEC pathogenesis and their influence on the transcription of *ler*, the activator of the LEE genes. Using Dulbecco's modified Eagle's medium (DMEM) lacking glucose and pyruvate as our base medium, we prepared assay media by adding glucose, glycerol, succinate, or pyruvate (Fig. 1A). Switching to glycolytic conditions by increasing concentrations of glucose (0.1% to 0.4%; 5.56 mM and 25 mM, respectively) or using 0.4% glycerol reduced *ler* transcription 2-fold, while switching to a gluconeogenic state with 0.4% succinate increased *ler* mRNA levels 4-fold compared to those with a glucose concentration of 0.4%. The switch from 0.1 to 0.4% glucose that alters virulence gene expression has been shown to be physiologically relevant in humans, where in cholesterol studies the use of 0.4% versus 0.1% glucose has been shown to increase the stimulation of cholesterol absorption in the small intestine (23). EHEC was unable to grow in 0.4% pyruvate as the sole carbon source, but adding it to 0.1% glucose did not vary *ler* transcription. These data indicate that transcription of the LEE is repressed under glycolytic conditions and activated under gluconeogenic conditions. These findings can be extended to other LEE-containing enteric pathogens, namely, enteropathogenic *E. coli* (EPEC) and *Citrobacter rodentium*, in which expression of the LEE genes is also reduced under glycolytic conditions (see Fig. S1 in the supplemental material).

To assess whether this carbon source regulation was linked to the QseC/KdpE-dependent LEE regulation, we assessed whether KdpE LEE gene regulation was affected under glycolytic or gluconeogenic conditions. Transcription of *ler* was decreased in the *kdpE* mutant compared to that in the wild type (WT) only at 0.1% glucose (gluconeogenic), and was similar to that of the WT at 0.4% glucose (glycolytic), indicating that KdpE activates *ler* transcription only in gluconeogenic environments (Fig. 1B). These findings were confounding, given that it has been previously reported that under conditions of high glucose availability (glycolytic), IIA^{Ntr} is dephosphorylated and only in its dephosphorylated form binds to the KdpD HK (the cognate HK for KdpE), increasing its activity and consequently KdpE phosphorylation, leading to higher expression of the KdpE target genes *kdpFABC* (24). Hence, through this mechanism one would predict that KdpE would activate LEE transcription under glycolytic and not gluconeogenic conditions, which is the opposite of the phenotype that we observed. We then hypothesized that KdpE might regulate the LEE in a glucose-dependent manner through interaction with another transcription factor. It has been well documented that fluctuations in glucose levels lead to different levels of cAMP within bacterial cells, and one of the prominent transcription factors involved in this regulation is cAMP receptor protein (CRP) (25). The CRP binding consensus sequence is very well defined (25), and *in silico* analysis of the *ler* regulatory region did not predict any CRP binding sites. Moreover, transcription of a *ler*::*lacZ* fusion (−393 to +86 bp) was indistinguishable between WT and Δ*crp E. coli* K-12 (Fig. 1C), further suggesting that CRP is not involved in *ler* regulation. However, these analyses identified a putative consensus sequence for Cra (Fig. 1D), a transcription factor that senses changes in metabolite levels as cues to differentially regulate its target genes (22). Cra is a member of the LacI/GalR family that activates genes encoding gluconeogenic enzymes such as FBPase and inhibits genes encoding glycolytic enzymes such as phosphofructokinase (26, 27).

We confirmed that *ler* transcription was decreased in both Δ*cra* EHEC and Δ*cra E. coli* K-12 grown in 0.1% (low) glucose and that this phenotype could be rescued by expressing Cra in *trans* (Fig. 1D and E). Transcription levels of *ler* were similar between WT and Δ*cra* strains in 0.4% (high) glucose (Fig. 1B and E), suggesting that Cra-dependent activation of *ler* also occurs only in low glucose. To confirm the predicted Cra binding site around −350 bp (Fig. 1D), we performed electrophoretic mobility shift assays (EMSAs) using a *ler* probe (−450 to −255 bp) (Fig. 1D and F). A Cra concentration of 7 nM was sufficient to shift the *ler* probe, while the negative-control probe *kan* did not shift with up to 10 μM Cra (Fig. 1F). To confirm specificity, competition EMSAs showed that Cra binding to *ler* could be competed by an unlabeled *ler* probe with a ratio as low as 1:1 but not by the nonspecific unlabeled *kan* probe (Fig. 1G). Using DNase protection assays, we verified the specific nucleotides in the *ler* promoter recognized by Cra (Fig. 2) and confirmed that Cra binds to its *in silico* predicted binding site.

Cra binding to its targets can be displaced by micromolar amounts of F1P or millimolar amounts of FBP (21, 56, 57). F1P and FBP are intermediates of the glycolysis metabolic pathway (Fig. 3A) (28). FBP is produced either through the glucose phosphorylation metabolic pathway or by the phosphorylation of F1P. To assess the role that glucose and/or its catabolites play in the binding of Cra to the *ler* promoter, EMSAs were performed with

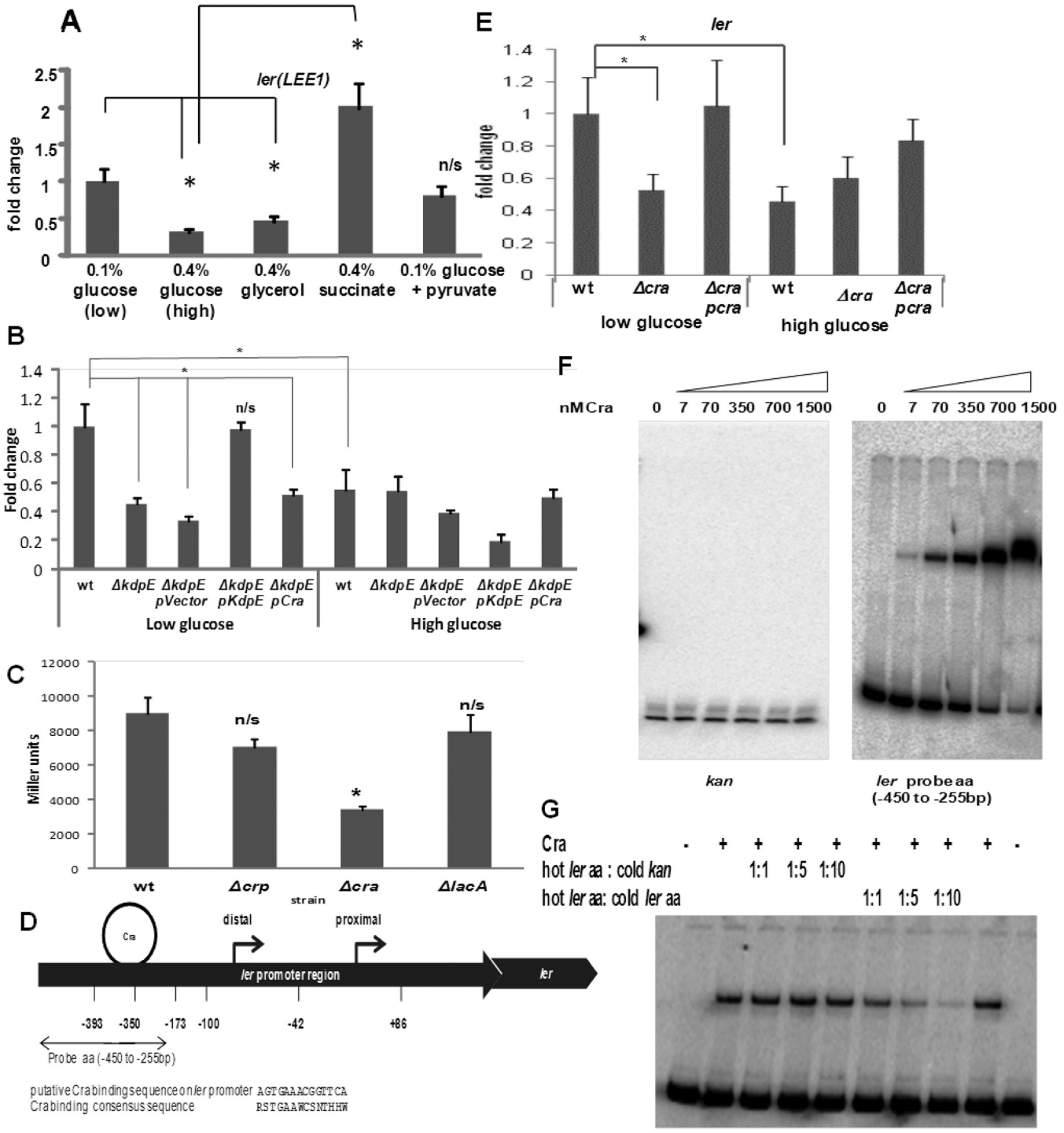

FIG 1 Carbon regulation of EHEC pathogenesis. (A) qRT-PCR of *ler* in the following media: no-glucose, no-pyruvate DMEM as the base medium supplemented with low glucose (0.1%), high glucose (0.4%), glycerol (0.4%), succinate (0.4%), or low glucose plus pyruvate (0.1% glucose + 0.4% pyruvate). Results were expressed as fold changes over those of low-glucose DMEM. n/s, not significant. *, $P < 0.05$. (B) qRT-PCR analysis of *ler* in WT and Δ*kdpE* strains complemented with either KdpE or Cra in low- and high-glucose DMEM. (C) Beta-galactosidase assays performed on *E. coli* K-12 strain BW2511 and its isogenic Δ*crp*, Δ*cra*, and Δ*lacA* mutants (from the Keio *E. coli* knockout library) transformed with plasmid pVS232Z (*ler-lacZ*, −393 to +86 bp) grown to an OD_{600} of 0.5 in low-glucose DMEM (contains 1 mM pyruvate and 0.1 M NaCl). (D) Schematic representation of the EHEC *ler* promoter. The transcriptional start sites are indicated with solid arrows. The putative binding site for Cra is depicted with a circle. Probe aa (−450 to −255 bp) was used in subsequent experiments. Underneath is the putative Cra binding sequence on the *ler* promoter and the Cra binding consensus sequence. (E) qRT-PCR of *ler* in WT and Δ*cra* strains and the complement in low- and high-glucose DMEM. *ler* transcript levels were quantified as fold differences normalized to low-glucose WT *ler* transcript levels. (F) Cra EMSA using probe aa. A radiolabeled *kan* DNA probe was used as a negative control. (G) Competition EMSA using 70 nM recombinant Cra and increasing amounts of unlabeled *ler* or *kan* probes.

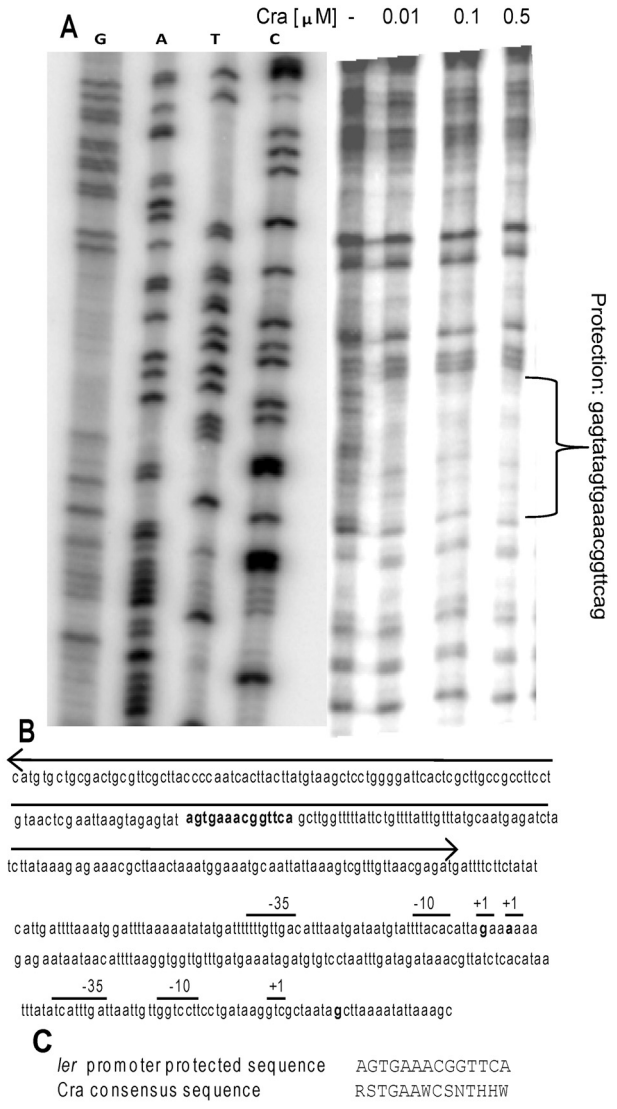

FIG 2 Footprinting of Cra on *ler*. (A) To identify the actual nucleotides of the *ler* promoter involved in binding with Cra, a DNase I footprint assay was carried out using increasing amounts of Cra. The protected region is indicated within the parentheses. (B) DNA sequence of the *ler* promoter region showing the −35 and −10 positions of both the proximal and distal promoters. The arrow shows the position of probe aa (containing the Cra binding region used in the EMSA studies), and the Cra binding site is indicated in bold. (C) Alignment of the actual binding site with the consensus binding site sequence of Cra.

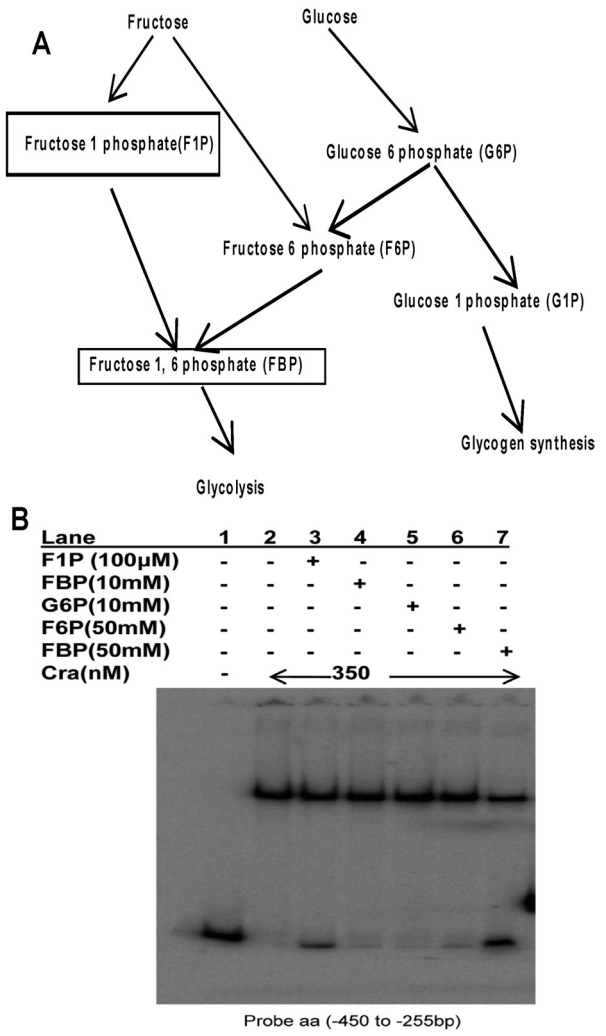

FIG 3 Catabolite regulation of Cra binding to DNA. (A) Schematic representation of glucose and fructose metabolism. The catabolites known to be inducers of Cra are boxed. (B) Inducer-supplemented EMSA. Indicated concentrations of intermediates in the fructose and glucose metabolism cascade were added to 2 ng (400 pM) radiolabeled *ler* probe (bp −450 to −255) and 70 nM Cra. G6P and F6P were used as negative controls.

100 μM F1P and 10 mM and 50 mM FBP. Fructose-6-phosphate (F6P) and glucose-6-phosphate (G6P) were used as negative controls. At a concentration of 350 nM, Cra completely shifted the *ler* probe (Fig. 3B). Addition of 100 μM F1P significantly reduced this shift, bringing the amount of free DNA in the reaction mixture to about 25% of the original protein free reaction mixture in lane 1 of Fig. 3B. For FBP, a 50 mM concentration was sufficient to decrease binding, bringing the amount of free DNA to approximately 50% (Fig. 3B). The ability of the glucose catabolite FBP to inhibit binding of Cra to *ler in vitro* may mirror FBP's role *in vivo* as a negative inducer of the Cra-*ler* complex formation. These results support the idea that Cra directly and specifically binds to the *ler* promoter region and that this binding is inhibited by metabolites such as F1P and FBP that accumulate under glycolytic conditions. Increasing the glucose concentration in the medium pushes the cell toward glycolytic metabolism that increases the amount of FBP in the cell. This would favor *ler* inhibition through the reduction of Cra binding. The switch to gluconeogenic metabolism using succinate decreases the amount of FBP available in the cell. This would promote Cra binding and increase *ler* transcription (Fig. 1A).

EHEC is a GI pathogen, *Bacteroides thetaiotaomicron* is a predominant species within the GI microbiota (29), and EHEC is likely to encounter a large population of this organism in the intestine. Hence, we investigated whether this sugar-dependent regulation of the LEE genes through Cra also occurs when EHEC is cocultured with *B. thetaiotaomicron* (Fig. 4), conditions that would more closely mimic the multibacterial species environment of the GI tract. Expression of the LEE gene *espA* is also higher in low glucose than in high glucose in the presence of *B. thetaiotao-*

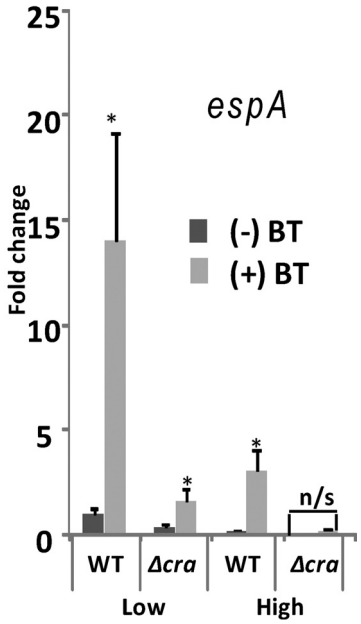

FIG 4 qRT-PCR of *espA* in high and low glucose for mixed populations of EHEC and *B. thetaiotaomicron* (1:9). EHEC WT and Δ*cra* strains were cocultured with *B. thetaiotaomicron*, and the transcription of *espA* was evaluated. *rpoA* mRNA levels were used as an internal control to normalize the output C_T values to take into account variation in bacterial numbers. *, $P < 0.05$; n/s, not significant.

micron, and Cra is still necessary for activation of its expression (Fig. 4). We have previously reported that the human microbiota produces the AI-3 signal (13) and proposed that EHEC, given its low infection dose, would not sense self-produced AI-3 in the initial stages of infection but sense the AI-3 produced by the intestinal microbiota (30). Indeed, coculture with *B. thetaiotaomicron* increased LEE gene expression in EHEC (Fig. 4), further substantiating our hypothesis that flora-produced AI-3 activates LEE expression.

Cra and KdpE interplay in LEE regulation. KdpE and Cra follow similar patterns toward sugar-dependent regulation of LEE expression, suggesting that these two transcription factors work together to integrate LEE regulation with signaling and metabolism. Through the genetic, bioinformatic, and biochemical analyses depicted in Fig. 1 and 2, we identified the Cra binding region within the *ler* promoter. Unlike Cra, which has a very well defined consensus sequence, KdpE tends to bind primarily to AT-rich DNA and does not have a very well defined consensus. Hence, to address the mechanism of KdpE-dependent *ler* regulation, we performed nested deletion analyses of the *ler* regulatory region (Fig. 5A). This deletion analysis narrowed the region of the *ler* promoter necessary for KdpE-dependent activation to between −173 and −42 bp (Fig. 5A and B). KdpE activates transcription of *ler* by directly binding to the *ler* regulatory region (Fig. 5C and D), and this interaction is specific, given that in a competition EMSA (Fig. 5E), unlabeled *ler* probe was able to compete with the labeled *ler* probe for KdpE binding but unlabeled *kan* probe (negative control) was unable to compete. Interestingly, the unphosphorylated KdpE showed higher binding affinity to the *ler* promoter than did the phosphorylated KdpE (Fig. 5F). This is in contrast to the KdpE regulation of the *kdpFABC* genes, to which the phosphorylated KdpE has higher binding affinity (24). During glycolytic growth, there is high glucose availability, IIA^{Ntr} is dephosphorylated and binds to the KdpD HK to increase KdpE phosphorylation (24), and as a result there is increased *kdpFABC* transcription and decreased KdpE-dependent LEE expression (Fig. 1B), given that the phosphorylated form of KdpE has lower affinity to the *ler* promoter (Fig. 5F). These results are in agreement with the observation that KdpE activates *ler* transcription only under gluconeogenic (low-glucose) conditions (Fig. 1B). Here, we defined that KdpE activates LEE transcription by binding within the bp −173 and −42 region, while Cra binds upstream to the bp −393 and −255 region (Fig. 1 to 5), and that under glycolytic conditions binding of both proteins to the *ler* promoter is diminished.

How these two transcription factors act in concert to activate *ler* expression remains undefined. Protein-protein interactions are an important mechanism for molecular processes in the cell. Different members of the LacI family have been shown to form homomultimers and to also interact with other proteins and metabolites as part of their regulatory mechanism (18, 56, 57). Since both KdpE and Cra activate *ler* transcription in a glucose-dependent manner, by directly binding the *ler* promoter, we investigated the possibility that Cra and KdpE interact with each other using far-Western blotting (FWB). His-tagged Cra, KdpE, and, as a negative control, QseB were run on gels, transferred to membranes, and then probed with whole-cell lysate (wcl) of a Δ*kdpE* Δ*cra* mutant expressing either Flag-tagged Cra or Flag-tagged KdpE. Duplicate membranes were then washed and probed with either anti-His or anti-Flag antibody. As expected, all three pure proteins were detected using anti-His-tag antibody (see Fig. S2 in the supplemental material). However, when wcl overexpressing Flag-tagged Cra was used to probe the membranes, only the lanes containing His-tagged Cra and His-tagged KdpE were detected with anti-Flag antibody, indicating that Flag-tagged Cra interacts with itself and KdpE but not with the negative control QseB (Fig. 6A). To further confirm this interaction, we reversed the bait-prey proteins (Fig. 6B). The wcl overexpressing Flag-tagged KdpE interacted with His-tagged KdpE as well as with Cra but not the control QseB. As additional negative controls, we either left replicate membranes unprobed by wcl or probed replicate membranes with the double mutant wcl only before probing with anti-Flag (see Fig. S2). These findings suggest that the two *ler*-activating proteins Cra and KdpE interact *in vitro*.

As Cra has previously been shown to enhance CRP binding to its targets (27), we examined whether Cra could have a similar effect on KdpE binding to *ler*. Using probe bb (−255 to −5 bp), which lacks the identified Cra binding site (Fig. 6C), we conducted mixed EMSAs where the KdpE concentration was kept constant and the Cra concentration was varied (Fig. 6D). We also repeated this assay, keeping the Cra concentration constant and varying the concentration of KdpE (Fig. 6E). When the concentration of KdpE was kept constant (Fig. 6D, lanes 4 to 7), we observed an increase in the amount of DNA shifted with increasing concentrations of Cra. The maximum amount of Cra added (1.5 μM, Fig. 6D, lane 3) was not sufficient to shift this probe on its own, but when supplemented with 2.5 μM KdpE, it significantly altered the shifting pattern compared to a reaction mixture with 2.5 μM KdpE only (lane 4). When this experiment was repeated keeping Cra constant and adding increasing amounts of KdpE, we again observed a supershift (Fig. 6E). These results indicate that the two proteins Cra and KdpE interact with each other to promote *ler*

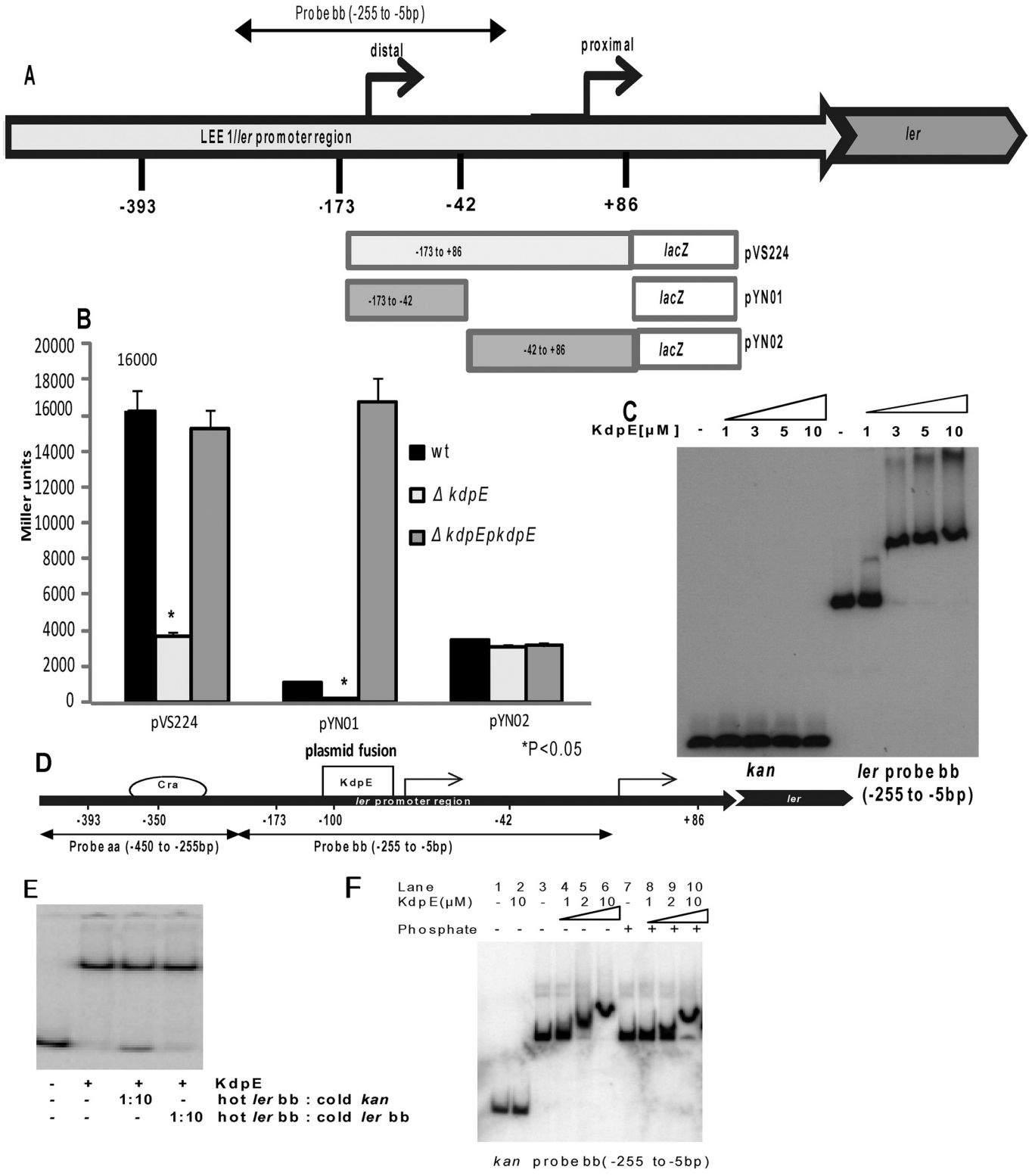

FIG 5 KdpE regulation of the *ler* promoter. (A) Cartoon representation of plasmids used for nested deletion analysis. Fragments of the *ler* regulatory region encompass the distal promoter (−173 to −42 bp, pYN01), proximal promoter (−42 to +86 bp, pYN02), and both promoters (−173 to +86 bp, pVS224). (B) Nested deletion analysis in WT and Δ*kdpE* strains and the complement. The beta-galactosidase assays were performed on samples grown to an OD_{600} of 0.5 in low-glucose DMEM (containing 1 mM pyruvate and 0.1 M NaCl). (C) KdpE EMSA of the *ler* promoter region using 2 ng (300 pM) probe bb (−255 to −5 bp). Increasing amounts of His-purified recombinant KdpE were used to shift the radiolabeled *ler* DNA probe. A radiolabeled *kan* DNA probe was used as a negative control. (D) Cartoon depicting the Cra and KdpE binding regions on *ler* and probes aa and bb used for EMSAs. (E) Competition EMSA using 5 μM recombinant KdpE and probe bb. A ratio of hot probe to cold probe of 1:10 decreased the shift due to 5 μM KdpE. Unlabeled *kan* DNA probe was used as a negative control. (F) EMSAs of KdpE and *ler* in the absence and presence of acetyl phosphate. *, $P < 0.05$.

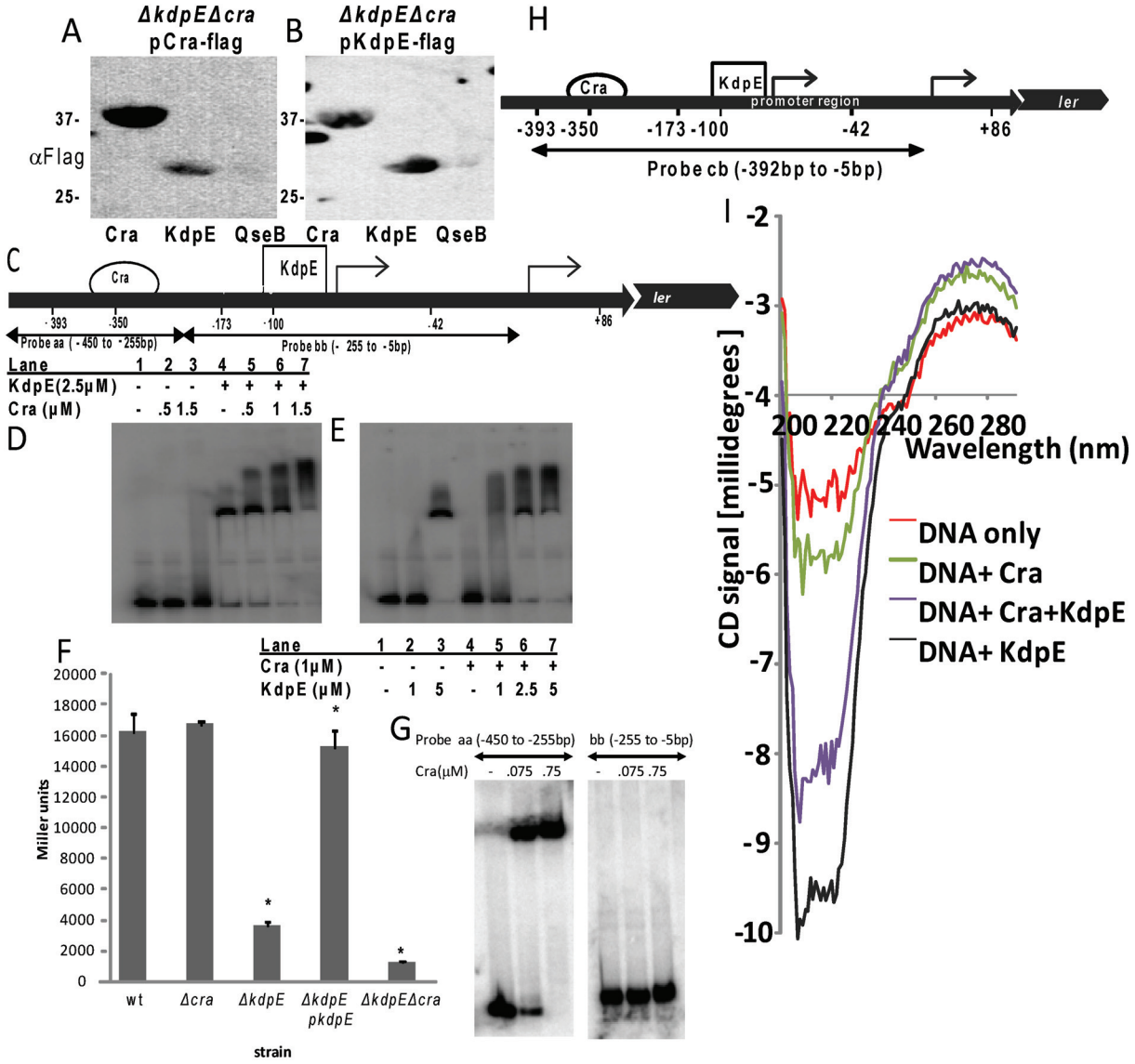

FIG 6 Cra and KdpE proteins interact *in vitro*. (A and B) Far-Western blotting of the interaction between Cra and KdpE *in vitro*. Recombinant His-tagged Cra, KdpE, and QseB (negative control) on a membrane were probed first with whole-cell lysate (wcl) overexpressing Flag-tagged Cra or Flag-tagged KdpE and then with anti-Flag antibodies. Cra is 37 kDa; KdpE and QseB are both 25 kDa. Bands indicate interaction between the membrane-bound His-tagged protein (bait) and the probing Flag-tagged protein (prey). Flag-Cra interacted with His-Cra and His-KdpE but not His-QseB (A). Flag-KdpE interacted with His-Cra and His-KdpE but not His-QseB (B). (C) Cartoon depicting the Cra and KdpE binding regions on *ler* and probes aa and bb used for EMSAs. (D and E) Mixed protein competition EMSAs were performed using probe bb (−255 to −5 bp). The EMSAs were performed with a constant concentration of KdpE and increasing concentrations of Cra (D) or with a constant concentration of Cra and increasing concentrations of KdpE (E). (F) Beta-galactosidase measurements of *ler-lacZ* fusion pVS224 (lacking the Cra binding site) in WT, Δ*cra*, and Δ*kdpE* strains and complement and Δ*kdpE* Δ*cra* strains. *, $P < 0.05$. (G) EMSAs of the *ler* probes aa and bb with Cra. (H) Schematic representation of EHEC *ler* promoter region indicating the Cra and KdpE binding sites and position of the probe cb (−392 to −5 bp) used for the CD assay. (I) CD spectra were recorded from 190 nm to 290 nm in 1-nm steps using a 1-mm-path-length cell. Samples in 50 mM phosphate buffer (pH 8, 25°C) were scanned three times and averaged for DNA only (red), DNA plus Cra (green), DNA plus KdpE (black), and DNA plus Cra plus KdpE (purple). The changes observed between 240 and 280 nm indicate DNA conformational changes due to the addition of protein.

transcription. To further test whether the effect of Cra enhancement of KdpE binding could enhance KdpE-dependent *ler* transcription, we utilized a *ler-lacZ* fusion, pVS224 (Fig. 5A), containing only the bp −173 to +86 region (which lacks the Cra binding region, Fig. 6C and G) to monitor KdpE-dependent *ler* transcription in the absence or presence of Cra. As predicted, transcription of this *ler-lacZ* fusion was unaffected in the *cra* mutant compared to that in WT (Fig. 6F), given that Cra does not interact with this region of the *ler* promoter (Fig. 6D and G). In agreement with our nested deletion analyses (Fig. 5), transcription of this fusion was decreased in the *kdpE* mutant and decreased even further in the double *kdpE cra* mutant (Fig. 6F), suggesting that interaction between Cra and KdpE has an additive effect on the expression of *ler*. However, these proteins bind to the *ler* regulatory region at sites that are distant from one another (Fig. 1 to 5), suggesting that in order for them to interact there has to be DNA bending and loop-

ing. Using circular dichroism (CD), we observed that binding of KdpE to the *ler* promoter slightly changes the DNA structure, while binding of Cra causes a much bigger change, and this change is exacerbated when the two proteins bind together (Fig. 6H and I). The LEE is a PI horizontally acquired by EHEC and has a very low GC content (34%) compared to the GC content of the *E. coli* backbone genome (50%) (32). It has also been extensively reported that because of this low-GC-content feature, the regulatory region of *ler* is prone to DNA bending (33), and *ler* transcription is subject to regulation by several architectural proteins that promote DNA bending such as H-NS, Fis, and Ihf (4). Hence, it is feasible that through DNA bending, Cra and KdpE interact to optimally activate *ler* transcription.

Cra and KdpE in AE lesion formation. Ler is the master activator of the *LEE* genes (Fig. 7A) (4). In low glucose, the decreased expression levels of the *LEE2*, *LEE3*, and *LEE5* operons in the *cra* and *kdpE* mutants were comparable (Fig. 7B), in agreement with the role of these two transcription factors in activating transcription of *ler* (Fig. 1 to 6). However, the mRNA level of *LEE4* (measured by *espA*, which encodes the T3SS translocon and which is itself secreted through the T3SS) was significantly decreased in the Δ*cra* strain but not in the Δ*kdpE* strain (Fig. 7B). It is worth noting that expression of the *LEE4* operon is also subject to high levels of posttranscriptional regulation (34) and that the RNA binding protein CsrA (involved in posttranscription carbon metabolism regulation [35–37]) differentially affects expression of *LEE4* (38). Hence, a potential explanation for the differential *LEE4* regulation between KdpE and Cra may be that in addition to modulating *ler* transcription, these proteins also differentially affect expression of posttranscriptional regulatory systems that exclusively act on *LEE4*. Transcription of *ler* is decreased in high glucose compared to that in low glucose, and this phenotype is mediated through both Cra and KdpE (Fig. 1 to 6). Switching to high glucose reduced *espA* transcription in the WT but did not affect the mRNA levels in the Δ*cra* and Δ*kdpE* mutants (Fig. 7C). Both the expression (Fig. 7D) and the secretion (Fig. 7E) of EspA were decreased in WT grown in high glucose. Although the Δ*kdpE* strain had levels of expression and secretion similar to those of WT in low glucose, these levels were unaffected by switching to high glucose. No EspA expression/secretion was observed in the Δ*cra* strain. Altogether, these results indicate that carbon sources influence LEE expression not only transcriptionally but also posttranscriptionally and that KdpE and Cra act in concert in the transcriptional regulation but differ in the posttranscriptional regulation.

As deletion of either *cra* or *kdpE* affects expression of the LEE that affects AE lesion formation, we next investigated whether deletion of these transcription factors would impact pedestal formation. HeLa cells were infected with wild type or the mutant strains, actin was stained with fluorescein isothiocyanate (FITC)-phalloidin (green), and HeLa nuclei and bacteria were stained with propidium iodide (red). Pedestals were visualized as brilliant green patches underneath red bacteria. Although the Δ*kdpE* mutant formed slightly fewer pedestals than did the WT, the Δ*cra* strain had significantly reduced pedestal formation, and this could be complemented by introduction of a plasmid carrying *cra* (Fig. 8). The observation that, in addition to decreased *LEE1* to *LEE3* and *LEE5* expression, the Δ*cra* mutant also has a severe decrease in EspA expression (Fig. 7B to E) while the Δ*kdpE* mutant does not may explain the disparity in pedestal formation between these two mutants. Deletion of both *kdpE* and *cra* led to an inability to form pedestals (Fig. 8). Expression of Cra alone could partially complement this defect, while expression of KdpE alone could not. Full complementation was achieved only when both proteins were expressed in the double mutant (Fig. 8B). These data further advocate a synergistic role for these two transcription factors in virulence regulation.

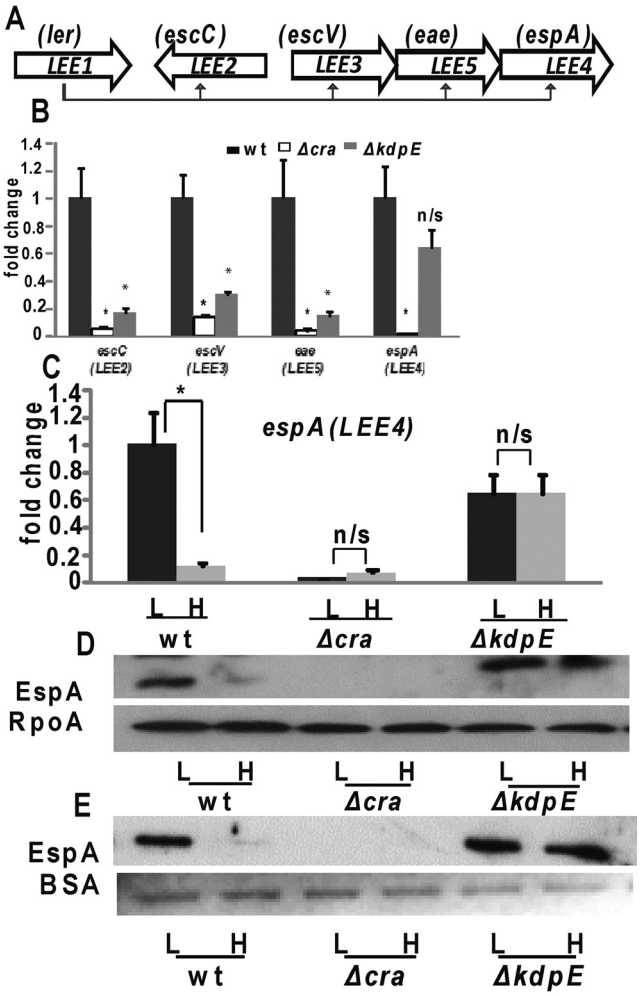

FIG 7 LEE regulation by Cra and KdpE. (A) Schematic representation of the LEE pathogenicity island. (B) qRT-PCR of the other LEE genes in low-glucose DMEM. The mutant mRNA levels were expressed as fold changes over WT mRNA levels. (C) qRT-PCR of *espA/LEE4* in WT, Δ*cra*, and Δ*kdpE* strains in low and high glucose. For all the samples, *rpoA* mRNA levels were used as an internal control to normalize the output C_T values in order to take into account variation in bacterial numbers. (D and E) Western blots of wcl (D) and SP (E) of WT, Δ*cra*, and Δ*kdpE* strains grown in low or high glucose were probed with antisera against EspA. RpoA and BSA were used as the loading controls for the wcl and SP blots, respectively. L, low glucose; H, high glucose. $P < 0.05$; n/s, nonsignificant.

Conclusions. The GI microbiota resides in the loose mucus layer and is not in close contact with the host epithelium (39). Growth within the GI tract is determined by the available concentration of nutrients. Consequently, for two species that compete for the same nutrients in the mucus layer and are not attached to the epithelial cells, the one that utilizes these nutrients more efficiently will eliminate the other strain (17). In the mammalian GI tract, EHEC has to compete with the gammaproteobacteria for

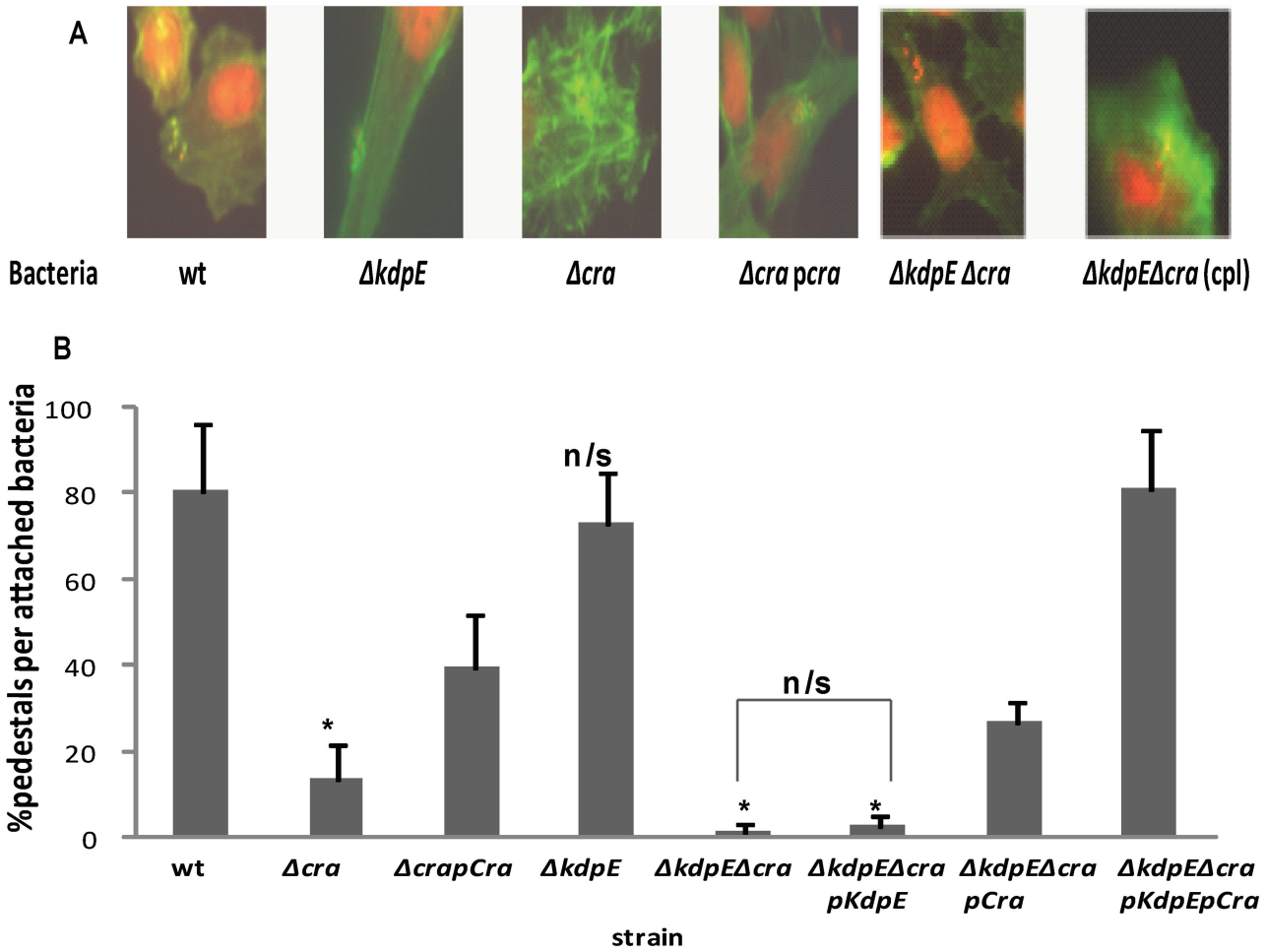

FIG 8 Cra and KdpE regulation in AE lesion formation. (A) Pedestals are green (actin) cups beneath red bacteria. (B) Quantification of pedestal formation. These were quantified (examining at least 50 HeLa cells per slide, 3 slides each) as percentages of pedestals per attached bacterium. The standard deviation is indicated in parentheses. *, $P < 0.05$; n/s, nonsignificant.

nutrients, because they have similar preferences for carbon source utilization. However, commensal *E. coli* is more proficient than EHEC in the utilization of these carbon sources. EHEC uses glycolytic substrates for initial growth but is unable to effectively compete for these carbon sources beyond the first few days and begins to utilize gluconeogenic substrates to stay within the intestine (17). A second strategy used by EHEC to establish colonization of the GI tract is the expression of the LEE-encoded T3SS to closely attach to the host enterocytes, leading to AE lesion formation (2). Activation of LEE expression relies on the sensing of the microbiota and host-derived signaling molecules AI-3 and epinephrine/norepinephrine through the QseC HK (6, 10, 13, 31). Upon sensing these signals, QseC initiates a complex signaling cascade, which through the phosphorylation of the KdpE RR leads to activation of the LEE genes (6). Here we show that optimal direct activation of *ler*, the master regulator of the LEE genes, by KdpE occurs in conjunction with Cra and that this regulation exclusively occurs under gluconeogenic conditions, showing that activation of the T3SS for epithelial attachment is coordinated with the gluconeogenic shift that EHEC undergoes during intestinal colonization of mammals (17).

Bacteria share common evolutionary progenitors. EHEC diverged from its nonpathogenic relatives about 4.5 million years ago (40), obtaining virulence traits, such as the LEE, through the insertion of mobile genetic elements (2, 41). Here we also show that through convergent evolution, two proteins that were originally designed to regulate nonpathogenic functions have been coopted by a pathogen to regulate virulence factors encoded within a horizontally acquired PI. This regulation also responds to differences in metabolite concentrations and the phosphorylation state of transcription factors, which can be modulated by the availability of carbon sources. This nutrient-based modulation of virulence expression is also intrinsically intertwined with interkingdom chemical signaling. In the GI tract environment, where about 1,000 different bacterial species coexist, the exquisite integration of different cues to regulate virulence gene expression is essential for an invading pathogen to successfully establish itself within a host.

MATERIALS AND METHODS

Strains and plasmids. Strains and plasmids are listed in Table S1 in the supplemental material. Standard molecular biology methods were used (42). Primers are listed in Table S2 in the supplemental material. Nonpolar mutants were constructed using λ-red (43). Briefly, for the construction of Δ*cra* and Δ*kdpE* Δ*cra* mutants (see Table S1), respectively, 86-24 (WT) and Δ*kdpE* cells containing pKD46 were prepared for electropora-

tion. A *cra* PCR product was amplified using JcraredF and JcraredR primers (see Table S2) with pKD4 as the template and then gel purified (Qiagen). The PCR product was then electroporated into the prepared cells and recovered in SOC medium for 6 h at 30°C and plated on LB containing kanamycin overnight at 42°C. Colonies were then screened for ampicillin sensitivity and kanamycin resistance and PCR verified using primers JcraexF and JcraexR for the absence of the gene. In order to create nonpolar mutants, the kanamycin cassette was resolved using the resolvase plasmid pCP20. The mutants were electroporated with pCP20, and resultant colonies were patched for kanamycin sensitivity. Final verification of proper deletion was performed by sequencing. The construction of the Δ*kdpE* mutant has been previously published (6).

Plasmids encoding recombinant proteins were constructed by amplifying the coding regions from the EHEC strain 86-24 using Phusion polymerase (NEB), digesting them with appropriate restriction enzymes (NEB), and ligating them into plasmids as summarized in Tables S1 and S2 in the supplemental material. Briefly, for the pBAD33-based plasmids pJN49 and pJN57, the primer pairs JkdpE33_2F/JkdpE33_2R and Jcra33F/Jcra33R were used to amplify the *kdpE* and *cra* genes, respectively, with strain 86-24 as a template. The resulting PCR products were cloned into the XbaI and HindIII cloning site of vector pBAD33 (44). To construct Flag-tagged versions of the above-described plasmids, the reverse primers were replaced with Jkdpe33flagR and Jcra33flagR and the cloning process was repeated to create pJN45 and pJN46, respectively. Plasmid pJN56 was constructed by amplifying the *cra* gene from strain 86-24 using primers JcramycF and JcramycR and cloning the PCR product into the KpnI and EcoRI cloning site of vector pBADMycHisA (Invitrogen). The protein expression plasmid pJN55 was constructed by amplifying the *cra* gene using primers Jcra21F and Jcra21R and cloning the resulting PCR product into the BamHI and NotI cloning site of vector pET21 (EMBD Biosciences). Proper cloning of the plasmids was confirmed by sequencing.

RNA extraction and qRT-PCR. Cultures were grown in DMEM to an optical density at 600 nm (OD_{600}) of 1.0. RNA from 3 replicates was extracted using the RiboPure bacterial isolation kit according to the manufacturer's protocols (Ambion). Quantitative reverse transcription-PCR (qRT-PCR) was performed as described previously (6). Briefly, diluted extracted RNA was mixed with validated primers (see Table S2 in the supplemental material), RNase inhibitor, and reverse transcriptase (AB). The mix was used in a one-step reaction utilizing an ABI 7500 sequence detection system. Data were collected using ABI Sequence Detection 1.2 software, normalized to endogenous *rpoA* levels, and analyzed using the comparative critical threshold (C_T) method. Analyzed data were presented as fold changes over WT levels. The Student unpaired *t* test was used to determine statistical significance. A *P* value of ≤0.05 was considered significant.

Nested deletion analysis. Reporter plasmids were constructed as previously described (47). For the construction of pYN01 and pYN02, the *ler* promoter region was amplified from the 86-24 strain, using the primer pairs Y2/R1 and Y1/R2, respectively. The resulting PCR products were then cloned into the BamHI and EcoRI cloning site of pRS551 (46). Construction of pVS224 has been previously published (47). The beta-galactosidase assays were performed as described previously (47). Briefly, appropriate strains containing different *lacZ* fusion-expressing plasmids (see Table S1 in the supplemental material) were grown overnight aerobically at 37°C in LB. Dilutions of 1:100 were grown in triplicate in clear DMEM (low glucose, 0.1 M salt, 0.001 M pyruvate) and appropriate antibiotics to mid-exponential phase (OD_{600} of 0.5). Cells were diluted in Z buffer and lysed with chloroform and 0.1% SDS. After addition of *o*-nitrophenyl-β-d-galactopyranoside (ONPG), the reaction was timed and stopped using 1 M Na_2CO_3. The OD_{420} was measured and used to calculate the Miller units as previously described (48). The Student unpaired *t* test was used to determine statistical significance. A *P* value of ≤0.05 was considered significant.

Protein purification, Western blotting, and FWB. pET21-based plasmids were induced with isopropyl-β-d-galactopyranoside (IPTG), and the proteins were purified using nickel columns (Qiagen). A modified protocol from the work of Wu et al. was used to perform far-Western blotting (FWB) assays (49). Briefly, equimolar amounts of purified His-tagged protein were separated on a 12% SDS gel, transferred, and blocked with 10% milk in Tris-buffered saline containing 0.05% Tween (TBST). Replicate membranes were then probed with whole-cell lysates (wcl) of the Δ*kdpE* Δ*cra* double mutant (negative control) or the double mutant overexpressing either Flag-tagged KdpE or Cra. As a further (negative) control, a replicate membrane was left unprobed by the wcl. All membranes were then probed with either anti-His or anti-Flag primary antibodies and then incubated with a secondary antibody conjugated to streptavidin-horseradish peroxidase (HRP). Enhanced chemiluminescence (ECL) reagent (GE) was added, and membranes were exposed to film to detect interacting proteins.

For Western blotting, wcl and secreted proteins (SP) were isolated as previously described (50). One hundred micrograms of bovine serum albumin (BSA) was added to SP for loading control.

EMSAs. EMSAs were performed as previously described (51). Briefly, defined regions of the promoter (see Text S1 and Table S2 in the supplemental material) were amplified by PCR, purified, quantified, and end labeled using radiolabeled [γ-^{32}P]ATP (PerkinElmer) and T4 polynucleotide kinase (NEB) according to the manufacturer's instructions. The radiolabeled probes were then repurified to remove unincorporated ATP. EMSAs were performed by adding increasing amounts of purified recombinant protein to 2 ng labeled probe in binding buffer [60 nM HEPES, pH 7.5, 5 mM EDTA, 3 mM dithiothreitol (DTT), 300 mM KCl, 25 mM $MgCl_2$, 50 ng poly(dI-dC), 500 μg/ml BSA (NEB)] (52). In relevant experiments, metabolites were added to the indicated final concentrations. The reaction mixtures were incubated for 20 min at room temperature and then loaded on a 6% polyacrylamide gel after addition of a 5% Ficoll DNA loading buffer. The gel was run at 180 V for 6 h or 50 V overnight, dried, and exposed on a phosphorimager.

DNase I protection (footprinting) assay. The footprinting assays were performed as previously described (52). Briefly, radiolabeled probes were made as described for the EMSAs. The binding reactions were also performed as described for the EMSAs. After the 20-min incubation, a 1:5 dilution of DNase I (Invitrogen) was added and allowed to digest unprotected DNA at room temperature for a set amount of time. The digestion was then stopped by adding 100 μl of stop buffer (200 mM NaCl, 2 mM EDTA, and 1% SDS). Protein was then removed using isoamyl-phenol-chloroform, and the DNA was precipitated using 3 M potassium acetate, 100% ethanol, and 1 μl glycogen. The concentrated samples and a sequencing reaction mixture (Epicentre) were then run on an 8% polyacrylamide gel, dried, and exposed on a phosphorimager. To generate the sequencing reaction, the initial PCR products were used as the template and amplified with end-labeled reverse primers according to the manufacturer's instructions.

Fluorescein actin staining assays. Assays were performed as described by Knutton et al. (54). Briefly, HeLa cells were grown on coverslips in wells containing DMEM supplemented with 10% fetal bovine serum (FBS) and 1% PSG antibiotic mix at 37°C, 5% CO_2, overnight to about 80% confluence. The wells were then thoroughly washed with phosphate-buffered saline (PBS) and replaced with fresh medium supplemented with arabinose (0.2% final concentration) and lacking antibiotics. Overnight static cultures of bacteria were then used to infect cells at a dilution of 100:1 (bacteria to DMEM). After a 6-h infection at 37°C, 5% CO_2, the coverslips were washed, fixed, and permeabilized. The samples were then treated with fluorescein

Isothiocyanate (FITC)-labeled phalloidin and propidium iodide were used to visualize actin accumulation and bacteria, respectively. Propidium iodide also stained HeLa nuclei red. The coverslips were then mounted on slides and visualized with a Zeiss Axiovert microscope. Pedestal formation was quantified as percentage of pedestals formed per at-

tached bacterium. Replicate coverslips from multiple experiments were quantified, and statistical analyses were performed using the Student *t* test. Serially diluted samples of the original bacterial cultures were also plated to confirm that similar CFU ratios were used for infection.

CD. Circular dichroism (CD) experiments were performed as previously described (55). CD curves were recorded on an Aviv model 62DS spectropolarimeter using a 1-mm-path-length cell. CD spectra were recorded from 190 nm to 290 nm in 1-nm steps in 50 mM phosphate buffer (pH 8, 25°C) on samples of the proteins Cra and KdpE and the *ler* promoter DNA fragment cb, which encompasses both the Cra and the KdpE binding site (−392 to −5 bp). Three scans were taken and averaged. The effect of proteins on DNA conformation was tracked between 240 nm and 280 nm, as most proteins show no significant CD spectrum in this wavelength range.

Coculture conditions. *B. thetaiotaomicron* VPI-5482 (ATCC 29148) was grown anaerobically overnight at 37°C in liquid TYG medium (59) plus 200 μg ml^{-1} gentamicin. Wild-type EHEC O157:H7 strain 86-24 and the isogenic Δ*cra* mutant were grown anaerobically overnight at 37°C in liquid LB plus 100 μg ml^{-1} gentamicin. The overnight cultures were pelleted and resuspended in either low-glucose DMEM or high-glucose DMEM (Invitrogen). *B. thetaiotaomicron* was plated in a 10-fold excess over EHEC O157:H7 to represent the composition of the intestinal microbiota. The bacteria were grown anaerobically in 12-well tissue culture plates in 2 ml of either low-glucose or high-glucose DMEM for 6 h in a GasPak EZ anaerobe container (Becton, Dickinson). RNA was extracted from three biological replicates using a RiboPure bacterial RNA isolation kit (Ambion) according to the manufacturer's guidelines.

SUPPLEMENTAL MATERIAL

Supplemental material for this article may be found at http://mbio.asm.org/lookup/suppl/doi:10.1128/mBio.00280-12/-/DCSupplemental.

Text S1, DOCX file, 0.1 MB.
Figure S1, DOCX file, 0.1 MB.
Figure S2, DOCX file, 0.1 MB.
Figure S3, DOCX file, 0.1 MB.
Table S1, DOCX file, 0.1 MB.
Table S2, DOCX file, 0.1 MB.

ACKNOWLEDGMENTS

We thank T. Conway (Oklahoma University) and L. Reitzer (UT Dallas) for advice on experimental design and analysis of the metabolism data. We thank Jose Rizo-Rey (UT Southwestern) for advice on the CD experiments.

This work was supported by NIH grant AI053067 and the Burroughs Wellcome Fund.

REFERENCES

1. **Gill SR, et al.** 2006. Metagenomic analysis of the human distal gut microbiome. Science **312**:1355–1359.
2. **Kaper JB, Nataro JP, Mobley HL.** 2004. Pathogenic *Escherichia coli*. Nat. Rev. Microbiol. **2**:123–140.
3. **Deng W, et al.** 2004. Dissecting virulence: systematic and functional analyses of a pathogenicity island. Proc. Natl. Acad. Sci. U. S. A. **101**:3597–3602.
4. **Mellies JL, Barron AM, Carmona AM.** 2007. Enteropathogenic and enterohemorrhagic *Escherichia coli* virulence gene regulation. Infect. Immun. **75**:4199–4210.
5. **Tobe T, et al.** 2006. An extensive repertoire of type III secretion effectors in *Escherichia coli* O157 and the role of lambdoid phages in their dissemination. Proc. Natl. Acad. Sci. U. S. A. **103**:14941–14946.
6. **Hughes DT, Clarke MB, Yamamoto K, Rasko DA, Sperandio V.** 2009. The QseC adrenergic signaling cascade in enterohemorrhagic *E. coli* (EHEC). PLoS Pathog. **5**:e1000553. http://dx.doi.org/10.1371/journal.ppat.1000553.
7. **Nakashima K, Sugiura A, Momoi H, Mizuno T.** 1992. Phosphotransfer signal transduction between two regulatory factors involved in the osmoregulated kdp operon in *Escherichia coli*. Mol. Microbiol. **6**:1777–1784.
8. **Sugiura A, Hirokawa K, Nakashima K, Mizuno T.** 1994. Signal-sensing mechanisms of the putative osmosensor KdpD in *Escherichia coli*. Mol. Microbiol. **14**:929–938.
9. **Sugiura A, Nakashima K, Mizuno T.** 1993. Sequence-directed DNA curvature in activator-binding sequence in the *Escherichia coli* kdp ABC promoter. Biosci. Biotechnol. Biochem. **57**:356–357.
10. **Clarke MB, Hughes DT, Zhu C, Boedeker EC, Sperandio V.** 2006. The QseC sensor kinase: a bacterial adrenergic receptor. Proc. Natl. Acad. Sci. U. S. A. **103**:10420–10425.
11. **Heermann R, et al.** 2009. The universal stress protein UspC scaffolds the KdpD/KdpE signaling cascade of *Escherichia coli* under salt stress. J. Mol. Biol. **386**:134–148.
12. **Jung K, Tjaden B, Altendorf K.** 1997. Purification, reconstitution, and characterization of KdpD, the turgor sensor of *Escherichia coli*. J. Biol. Chem. **272**:10847–10852.
13. **Sperandio V, Torres AG, Jarvis B, Nataro JP, Kaper JB.** 2003. Bacteria-host communication: the language of hormones. Proc. Natl. Acad. Sci. U. S. A. **100**:8951–8956.
14. **Chang DE, et al.** 2004. Carbon nutrition of *Escherichia coli* in the mouse intestine. Proc. Natl. Acad. Sci. U. S. A. **101**:7427–7432.
15. **Fabich AJ, et al.** 2008. Comparison of carbon nutrition for pathogenic and commensal *Escherichia coli* strains in the mouse intestine. Infect. Immun. **76**:1143–1152.
16. **Jones SA, et al.** 2008. Glycogen and maltose utilization by *Escherichia coli* O157:H7 in the mouse intestine. Infect. Immun. **76**:2531–2540.
17. **Miranda RL, et al.** 2004. Glycolytic and gluconeogenic growth of *Escherichia coli* O157:H7 (EDL933) and *E. coli* K-12 (MG1655) in the mouse intestine. Infect. Immun. **72**:1666–1676.
18. **Ramseier TM, et al.** 1993. *In vitro* binding of the pleiotropic transcriptional regulatory protein, FruR, to the fru, pps, ace, pts and icd operons of *Escherichia coli* and *Salmonella typhimurium*. J. Mol. Biol. **234**:28–44.
19. **Gore AL, Payne SM.** 2010. CsrA and Cra influence *Shigella flexneri* pathogenesis. Infect. Immun. **78**:4674–4682.
20. **Yoon H, McDermott JE, Porwollik S, McClelland M, Heffron F.** 2009. Coordinated regulation of virulence during systemic infection of *Salmonella enterica* serovar typhimurium. PLoS Pathog. **5**:e1000306. http://dx.doi.org/10.1371/journal.ppat.1000306.
21. **Ramseier TM, Bledig S, Michotey V, Feghali R, Saier MH, Jr.** 1995. The global regulatory protein FruR modulates the direction of carbon flow in *Escherichia coli*. Mol. Microbiol. **16**:1157–1169.
22. **Saier MH, Jr, Ramseier TM.** 1996. The catabolite repressor/activator (Cra) protein of enteric bacteria. J. Bacteriol. **178**:3411–3417.
23. **Ravid Z, et al.** 2008. Modulation of intestinal cholesterol absorption by high glucose levels: impact on cholesterol transporters, regulatory enzymes, and transcription factors. Am. J. Physiol. Gastrointest. Liver Physiol. **295**:G873–G885.
24. **Lüttmann D, et al.** 2009. Stimulation of the potassium sensor KdpD kinase activity by interaction with the phosphotransferase protein IIA(Ntr) in *Escherichia coli*. Mol. Microbiol. **72**:978–994.
25. **Hengge-Aronis R.** 1999. Interplay of global regulators and cell physiology in the general stress response of *Escherichia coli*. Curr. Opin. Microbiol. **2**:148–152.
26. **Chin AM, Feldheim DA, Saier MH, Jr.** 1989. Altered transcriptional patterns affecting several metabolic pathways in strains of *Salmonella typhimurium* which overexpress the fructose regulon. J. Bacteriol. **171**:2424–2434.
27. **Ryu S, Ramseier TM, Michotey V, Saier MH, Jr, Garges S.** 1995. Effect of the FruR regulator on transcription of the pts operon in *Escherichia coli*. J. Biol. Chem. **270**:2489–2496.
28. **Romano AH, Conway T.** 1996. Evolution of carbohydrate metabolic pathways. Res. Microbiol. **147**:448–455.
29. **Hooper LV, et al.** 2001. Molecular analysis of commensal host-microbial relationships in the intestine. Science **291**:881–884.
30. **Sperandio V, Mellies JL, Nguyen W, Shin S, Kaper JB.** 1999. Quorum sensing controls expression of the type III secretion gene transcription and protein secretion in enterohemorrhagic and enteropathogenic *Escherichia coli*. Proc. Natl. Acad. Sci. U. S. A. **96**:15196–15201.
31. **Rasko DA, et al.** 2008. Targeting QseC signaling and virulence for antibiotic development. Science **321**:1078–1080.
32. **Elliott SJ, et al.** 1998. The complete sequence of the locus of enterocyte effacement (LEE) from enteropathogenic *Escherichia coli* E2348/69. Mol. Microbiol. **28**:1–4.
33. **Yoon JW, et al.** 2004. Thermoregulation of the *Escherichia coli* O157:H7

pO157 ecf operon and lipid A myristoyl transferase activity involves intrinsically curved DNA. Mol. Microbiol. **51**:419–435.
34. **Lodato PB, Kaper JB.** 2009. Post-transcriptional processing of the LEE4 operon in enterohaemorrhagic *Escherichia coli*. Mol. Microbiol. **71**: 273–290.
35. **Romeo T.** 1996. Post-transcriptional regulation of bacterial carbohydrate metabolism: evidence that the gene product CsrA is a global mRNA decay factor. Res. Microbiol. **147**:505–512.
36. **Romeo T, Gong M, Liu MY, Brun-Zinkernagel AM.** 1993. Identification and molecular characterization of csrA, a pleiotropic gene from *Escherichia coli* that affects glycogen biosynthesis, gluconeogenesis, cell size, and surface properties. J. Bacteriol. **175**:4744–4755.
37. **Sabnis NA, Yang H, Romeo T.** 1995. Pleiotropic regulation of central carbohydrate metabolism in *Escherichia coli* via the gene csrA. J. Biol. Chem. **270**:29096–29104.
38. **Bhatt S, et al.** 2009. The RNA binding protein CsrA is a pleiotropic regulator of the locus of enterocyte effacement pathogenicity island of enteropathogenic *Escherichia coli*. Infect. Immun. **77**:3552–3568.
39. **Vaishnava S, et al.** 2011. The antibacterial lectin RegIIIgamma promotes the spatial segregation of microbiota and host in the intestine. Science **334**:255–258.
40. **Reid SD, Herbelin CJ, Bumbaugh AC, Selander RK, Whittam TS.** 2000. Parallel evolution of virulence in pathogenic *Escherichia coli*. Nature **406**: 64–67.
41. **Ahmed N, Dobrindt U, Hacker J, Hasnain SE.** 2008. Genomic fluidity and pathogenic bacteria: applications in diagnostics, epidemiology and intervention. Nat. Rev. Microbiol. **6**:387–394.
42. **Sambrook J, Fritsch EF, Maniatis T.** 1989. Molecular cloning: a laboratory manual, 2nd ed. Cold Spring Harbor Laboratory Press, Cold Spring Harbor, NY.
43. **Datsenko KA, Wanner BL.** 2000. One-step inactivation of chromosomal genes in *Escherichia coli* K-12 using PCR products. Proc. Natl. Acad. Sci. U. S. A. **97**:6640–6645.
44. **Guzman LM, Belin D, Carson MJ, Beckwith J.** 1995. Tight regulation, modulation, and high-level expression by vectors containing the arabinose PBAD promoter. J. Bacteriol. **177**:4121–4130.
45. Reference deleted.
46. **Simons RW, Houman F, Kleckner N.** 1987. Improved single and multicopy lac-based cloning vectors for protein and operon fusions. Gene **53**: 85–96.
47. **Sharp FC, Sperandio V.** 2007. QseA directly activates transcription of LEE1 in enterohemorrhagic *Escherichia coli*. Infect. Immun. **75**: 2432–2440.
48. **Miller JH.** 1972. Experiments in molecular genetics. Cold Spring Harbor Laboratory Press, Cold Spring Harbor, NY.
49. **Wu Y, Li Q, Chen XZ.** 2007. Detecting protein-protein interactions by Far western blotting. Nat. Protoc. **2**:3278–3284.
50. **Jarvis KG, et al.** 1995. Enteropathogenic *Escherichia coli* contains a putative type III secretion system necessary for the export of proteins involved in attaching and effacing lesion formation. Proc. Natl. Acad. Sci. U. S. A. **92**:7996–8000.
51. **Kendall MM, Rasko DA, Sperandio V.** 2010. The LysR-type regulator QseA regulates both characterized and putative virulence genes in enterohaemorrhagic *Escherichia coli* O157:H7. Mol. Microbiol. **76**:1306–1321.
52. **Clarke MB, Sperandio V.** 2005. Transcriptional autoregulation by quorum sensing *Escherichia coli* regulators B and C (QseBC) in enterohaemorrhagic *E. coli* (EHEC). Mol. Microbiol. **58**:441–455.
53. Reference deleted.
54. **Knutton S, Baldwin T, Williams PH, McNeish AS.** 1989. Actin accumulation at sites of bacterial adhesion to tissue culture cells: basis of a new diagnostic test for enteropathogenic and enterohemorrhagic *Escherichia coli*. Infect. Immun. **57**:1290–1298.
55. **Cary PD, Kneale GG.** 2009. Circular dichroism for the analysis of protein-DNA interactions. Methods Mol. Biol. **543**:613–624.
56. **Fujita Y, Miwa Y, Galinier A, Deutscher J.** 1995. Specific recognition of the *Bacillus subtilis* gnt cis-acting catabolite-responsive element by a protein complex formed between CcpA and seryl-phosphorylated HPr. Mol. Microbiol. **17**:953–960.
57. **Schumacher MA, Seidel G, Hillen W, Brennan RG.** 2007. Structural mechanism for the fine-tuning of CcpA function by the small molecule effectors glucose 6-phosphate and fructose 1,6-bisphosphate. J. Mol. Biol. **368**:1042–1050.
58. **Sperandio V, Torres AG, Kaper JB.** 2002. Quorum sensing *Escherichia coli* regulators B and C (QseBC): a novel two-component regulatory system involved in the regulation of flagella and motility by quorum sensing in *E. coli*. Mol. Microbiol. **43**:809–821.
59. **Betian HG, Linehan BA, Bryant MP, Holdeman LV.** 1977. Isolation of a cellulotytic *Bacteroides* sp. from human feces. Appl. Environ. **33**: 1009–1010.